Saidijam Massoud (Orcid ID: 0000-0002-1711-5619)

Synthesis, anticancer activity and β-lactoglobulin binding interactions of multi-targeted kinase inhibitor sorafenib tosylate (SORt) by spectroscopic and molecular modeling approaches

Hamid Tanzadehpanah [1], Asrin Bahmani [1], Neda Hosseinpour Moghadam [1], Hamid Gholami [2],

Hanie Mahaki [1], Abbas Farmany [3] and Massoud Saidijam[1,*]

[1] Research Center for Molecular Medicine, Hamadan University of Medical Sciences, Hamadan, Iran

[2] Department of Biochemistry, School of Medicine, Hamadan University of Medical Sciences, Hamadan, Iran

[3] Dental Research Center, School of Dentistry, Hamadan University of Medical Sciences, Hamadan, Iran.

*Corresponding author Email: Sjam110@yahoo.com

First author Email: H.Tanzadehpanah@gmail.com

Tel: +98 8138276299

This article has been accepted for publication and undergone full peer review but has not been through the copyediting, typesetting, pagination and proofreading process which may lead to differences between this version and the Version of Record. Please cite this article as doi: 10.1002/bio.3929

Abstract

Sorafenib tosylate (SORt) as an oral multi-kinase inhibitor is used for the treatment of advanced renal cell, liver and thyroid cancers. This drug was synthesized in this work, and its antiproliferative activities against HCT116 and CT26 cells were assessed. Afterward, the interaction of SORt with β-lactoglobulin (BLG) was studied using different fluorescence techniques, circular-dichroism (CD), zeta potential measurements and docking simulation. The results of IR, Mass, ^{H}NMR, and ^{C}NMR spectra exhibited that the drug was produced with a high quality, purity and efficiency. SORt showed potent cytotoxicity against HCT116 and CT26 cells with IC50 = 8.12 and 5.42 µM, respectively. Concerning the BLG binding of SORt; the results showed that a static quenching mechanism is the cause of high affinity for drug-protein interaction. Three-dimensional fluorescence and synchronous spectra proposed that SORt conformation has been changed at different levels, as well as circular dichroism suggested the amount of α-helix remains almost constant in the BLG–SORt complex, whereas those of random coil were decreased. The Zeta-potential values of BLG were more positive after binding with SORt, which is due to the existence of electrostatic interactions between BLG and SORt. Furthermore, thermodynamic parameters confirmed the van der Waals and hydrogen bond interactions in the complex formation. Finally, Molecular modeling showed the presence of hydrogen bond and electrostatic force in the BLG–SORt system, which was consistent with the experimental results.

Keywords: Sorafenib; β-lactoglobulin; MTT assay; Multi-spectroscopy; Docking.

Abbreviations

BLG: Beta-lactoglobulin

CD: Circular Dichroism

CDI: 4-chloro-3-(trifluoromethyl)aniline, N,N-carbonyldiimidazole

c-Kit: c-Kit protein

DMF: 4-Aminophenol, potassium tert-butylate, potassium carbonate, N,N-Dimethylformamide

FBS: fetal bovine serum

Flt-3: FMS-like tyrosine kinase 3

FT-IR: Fourier Transform Infrared

MOE: Molecular Operating Environment

NMR: Nuclear magnetic resonance

PDGFRβ: platelet-derived growth factor receptor β

SORt: sorafenib tosylate

VEGFR: vascular endothelial growth factor receptor

ΔG: standard Gibbs free energy change

ΔH: standard enthalpy change

ΔS: standard entropy change

Highlights

- ✓ Sorafenib tosylate (SORt) was synthesized with high quality, purity and efficiency.
- ✓ SORt showed potent cytotoxicity against HCT116 and CT26 colon cancer cells.
- ✓ Circular dichroism suggested the amount of α-helix remains almost constant in the BLG–SORt complex.
- ✓ Molecular modeling also showed the presence of hydrogen bond and electrostatic force in the BLG–SORt system.

1. Introduction

Colon cancer is a significant health problem, and by 2019, in the United States, it is anticipated that 101,420 people to contract the disease, which 51,020 will die [1]. A

convenient option for colon cancer treatment is oral consumption of Sorafenib tosylate (SORt). SORt an active multikinase inhibitor by affecting all three variants of vascular endothelial growth factor receptors (VEGFR 1, 2 and 3), FMS-like tyrosine kinase 3 (Flt-3), platelet-derived growth factor receptor β (PDGFRβ), c-Kit protein (c-Kit), and RET receptor tyrosine kinases induces its anti-cancer activity [2, 3]. Biological activities of SORt depend on its metabolism and bioavailability. Poor solubility in aqueous media limits the use of SORt as an efficient medicine. Therefore, it is necessary to use a suitable carrier to promote its activity [4].

Beta-lactoglobulin (BLG) is a typical globular protein with a molecular weight of 18.3 kDa and a size of nearly 2 nm [5]. In the sequence of this protein, there are two tryptophan residues (Trp-19 and Trp-61) that play a role in fluorescence spectroscopy studies as the main fluorophores [6]. The structure of BLG constitutes of nine antiparallel beta-strands that form two beta-sheets, and three turn's α-helix. The β-sheets form a flattened conical barrel named calyx, which is the center of interaction with small drugs [7]. BLG has six potential sites for ligand binding. The first site is the Calix position; the second site is between the beta strings C and D in the CD loop. The third site is formed by the alpha-helix c-terminal and the beta strands F, G, H and A. The fourth site is between Alpha-Helix and the beta-strand I. The fifth site is near Loop H. The sixth site is between the CD and DE loops [8]. Some studies have shown that β-lactoglobulin protein does not bind to any of the ligands through covalent bonding, and most bonds are hydrophobic and hydrogen interactions [9]. The result showed controlled release over a long period of time. Generally, when medications are taken orally, problems such as a broken stomach or irritation in the stomach appear. Therefore, there has always been an attempt to provide a molecule that can, while carrying the drug, allow it to pass intact through the stomach, eventually and release it into the target tissue (intestine) [10]. The structure of BLG is strongly dependent on the pH and ionic strength of the environment

due to the presence of many charged groups in its sequence. Resistant to low pH in the presence of pepsin degradation is another characteristic of BLG [11]. It remains wholesome after gastric digestion and can be detected in the small intestine and colon. This property of protein encouraged its use as a carrier for delivering drugs into the colon and developing a new drug delivery system in colon cancer treatment [12].

In the present study, we first synthesized SORt with high purity, and then its anti-cancer activity was investigated on two colon cancer cell lines of HCT116 and CT26. Furthermore, due to the unique properties of BLG, it can be a suitable carrier for SORt. So, we have focused on the interactions of SORt with BLG using fluorescence spectroscopy, circular dichroism, zeta potential measurement and molecular modeling, to use it in some drug delivery systems.

2. Martials, devices and methods

2.1. Martials

4-Aminophenol, potassium tert-butylate, potassium carbonate, N,N-Dimethylformamide (DMF), and p-toluenesulfonic acid were purchased from Merck (Darmstadt, Germany). 4-chloro-3-(trifluoromethyl)aniline, N,N-carbonyldiimidazole (CDI) and β-Lactoglobulin were obtained from Sigma (St. Louis, Mo, USA). 4-chloro-N-methyl-2-pyridinecarboxamide was bought from TCI (TCI America, Inc., Portland, OR, USA). HCT116 and CT26 cell lines were purchased from National Cell Bank, Pasteur Institute, Iran. The anticancer drug Regorafenib, used as a positive control in MTT assay, was purchased from Shaanxi Yuan Tai Biological Technology Co. Ltd, Xi'an City, PR China. All materials for cell culture were obtained from Gibco (Gibco, USA). Other materials were obtained from high-quality commercial suppliers and no additional purification was required.

2.2. Devices

All melting points were measured using Barnested/Electrothermal IA-9100 and values were uncorrected. Bruker FT-IR Alpha was used to identify the functional groups. NMR-Bruker-500-UltraSheild was used to analyze the number and types of C and H atoms. To obtain the mass spectra of the derivatives, Quadrupole technique and Agilent Technologies- 5975C- EI-70eV apparatus were used. All fluorescence spectra were achieved by employing a FP-6200 spectrofluorometer, with 1.0 cm quartz cells. An Aviv Model 215 Circular Dichroism spectrometer with a cell path length of 1cm, at room temperature, was used to the record of CD spectra. The zeta potential measurements were examined using a Zeta-sizer, Nano-series–ZS (Malvern Instruments Ltd).

2.3. Synthesis of sorafenib tosylate (SORt)

Synthesis of SORt was performed in 3 steps **(Scheme 1).**

2.3.1. Synthesis of 1-[4-Chloro-3-(trifluoromethyl) phenyl]-3-(4-hydroxyphenyl) urea

4-Chloro-3-(trifluoromethyl) aniline (1mmol) was added to the dichloromethane and was stirred until a clear solution was obtained. After 10 min, *N*,*N*-carbonyldiimidazole (1mmol) was added to the reaction mixture and the reaction was continued at reflux at 50°C. After 16 hours, the reaction was complete and 4-chloro-3-(trifluoromethyl) phenyl isocyanate was obtained (Scheme 1, route a). Then 4-aminophenol (1mmol) was added to the precursor product in dichloromethane. The reaction was continued at 25°C for 16h and finally, intermediate was obtained (Scheme 1, route b). Finally, the dichloromethane was distillated under reduced pressure and the intermediate was obtained as a white crystal without further purification.

2.3.2. Synthesis of 4-{4-[({[4-Chloro-3-(trifluoromethyl-phenyl]amino}carbonyl)amino] phenoxy}-*N*-methylpyridine-2-carboxamide (sorafenib)

The intermediate (1mmol) was dissolved in *N*,*N*-dimethylformamide. After the clear solution was obtained, potassium tert-butylate (1.5 mmol) was added to the reaction mixture and the reaction continued for 2h at 25°C. Then, 4-chloro-*N*-methyl-2-pyridinecarboxamide (1mmol) and potassium carbonate (0.5 mmol) were added to the reaction mixture. The reaction temperature was adjusted to about 80°C and the reaction continued for 8h. After 8 hours, the reaction was completed (Scheme 1, route c). To separate and purify the product, the reaction mixture was cooled to 25°C. The extraction process was then carried out by mixing water and ethyl acetate. The formed salts and polar components were dissolved in water and the non-polar components were dissolved in the nonpolar phase, namely ethyl acetate. Ethyl acetate was distillated under reduced pressure and sorafenib remained solid white.

2.3.3. Synthesis of 4-{4-[({[4-Chloro-3-(trifluoromethyl-phenyl]amino}carbonyl)amino] phenoxy}-*N*-methylpyridine-2-carboxamide tosylate (sorafenib tosylate)

Sorafenib (1mmol) was added to the ethanol and was stirred for 10 minutes until a clear solution was obtained. Subsequently, p-toluenesulfonic acid (1.1 mmol) was added to the reaction and stirred at 25°C for 15h (Scheme 1, route d). The solvent was distillated under reduced pressure and the final precipitate was washed several times with cold ethanol.

2.4. MTT assay

HCT116 and CT26 were grown in DMEM and RPMI 1640, respectively. The mediums were containing 10% fetal bovine serum (FBS) and 1% penicillin streptomycin. A humidified atmosphere incubator provides conditions of 95% air, 5% CO_2 and 37ºC for the cancer cells. To determine of cytotoxicity activity, about 4,000 cells were seeded into 96 well plates and incubated for 24 h. After incubation, the cells were treated with various concentrations of

SORt (0.5, 1, 2, 4, 8 and 16 µM) for three days. Then, MTT reagent was added to each well (fifteen microliters, 5 mg/ml) and the plates were incubated for 4 hours. The medium was removed and 150 µl DMSO was added to each well. After 20 minutes, the absorbance at 630 nm was measured [13, 14]. In MTT assay, regorafenib was employed as the positive control. Regorafenib, as a small molecule, has a chemical structure and biochemical profile similar to that of SORt. The only difference is the addition of a fluorine atom to the center of regorafenib, which increases its efficiency in anti-cancer activity. The cytotoxicity data were analyzed using one-way ANOVA followed by the post-hoc Tukey's test [15].

2.5. Fluorescence measurements

The measurements were done at a excitation wavelength of 280 nm, and the emission spectra were recorded from 290 to 450 nm [16]. Briefly, two milliliters of BLG (final concentration, 21×10^{-6} M) were titrated by serial addition of SORt (0 - 10×10^{-6} M), at 298, 305 and 310 temperatures and pH 7.4. In this study, the absorption of exciting light and reabsorption of emitted light were used to decrease the inner filter effect (IFE) using the following equation:

$$F_{cor} = F_{obs} \times exp^{(Aex+Aem)/2}$$

where F_{cor} and F_{obs} are the corrected and observed fluorescence intensities, respectively. A_{ex} and A_{em} are the absorption of SORt at the excitation and the emission wavelength, respectively.

Synchronous fluorescence spectra were assessed at two scanning intervals of $\Delta\lambda$ ($\Delta\lambda = \lambda_{em} - \lambda_{ex}$) [17]. $\Delta\lambda$ values were set at 15 and 60 nm. The concentrations of SORt and BLG were like the description above.

Excitation and emission wavelength ranges to estimate three-dimensional fluorescence spectra were 220 to 350 and 220 to 500 nm, respectively [18]. The final concentrations of SORt and BLG were 10×10^{-6} M and 21×10^{-6} M, respectively.

2.6. Circular dichroism (CD) spectroscopy

The CD spectra were obtained over a wavelength range of 200–260 nm, with a scanning rate at 50 nm min^{-1} as an average of two scans for each CD spectrum [19]. The concentration of BLG solution was 21×10^{-6} M, whereas the final concentrations of SORt in complex with BLG were 5×10^{-6} and 10×10^{-6} M.

2.7. Zeta potential measurements

The formation of the BLG-SORt complex can be further confirmed by the zeta potential measurements. One milliliter of BLG was prepared in 0.05 M phosphate buffer and room temperature (pH 7.4), that way, the final concentrations of BLG and SORt were 21×10^{-6} and $0.0 – 5 \times 10^{-6}$ M, respectively.

2.8. Molecular modeling

Molecular simulation based on blind docking was accomplished using Molecular Operating Environment (MOE) software [20]. ChemDraw Ultra software version 8.0 was applied for the SORt preparation. The geometry of SORt was optimized by applying HyperChem program version 7 (http://www.hyper.com). The crystal structure for BLG was obtained from the Protein Data Bank (PDB code: 2GJ5). First, all the water molecules were removed and hydrogen atoms were added to the protein file, as required in the Lamarckian Genetic Algorithm. The docking parameter file was set to 100 runs. Finally, the best docking energy result (the lowest energy) was assumed as the possible candidate for ligand-protein interaction and was used for the final analysis with the Discovery Studio Visualizer 2.5.5 and MOE softwares [21].

3. Results and discussions

3.1. Synthesis of sorafenib tosylate (SORt)

According to the general method and the synthetic details described in the preceding steps, the products were separated and purified at each step. Their physical properties and spectra information are reported below sections. It should be noted that the IR, Mass, ^{H}NMR, and ^{C}NMR spectra for SORt are presented in **Figures 1 and 2.**

3.1.1. Synthesis of 1-[4-Chloro-3-(trifluoromethyl) phenyl]-3-(4-hydroxyphenyl) urea

The Characterization of the target compound is described below.

White solid, Mp: 200°C, IR (KBr): υ (cm-1) = 3325-2500 (NH, OH), 1710 (C=O).

1H NMR (DMSO-d6): δ (ppm) = 7.17 (d, 3J= 8Hz, 2H-Ar), 7.59 (d, 3J=8Hz, 2H-Ar), 7.60 (d, 3J=8Hz, 1H-Ar), 7.70 (dd, 3J=8Hz, 4J=2.5Hz, 1H-Ar), 8.1 (d, 4J=2.5Hz, 1H-Ar), 9.39 (s, 1H, NH), 9.56 (s, 1H, NH).

13C NMR (DMSO-d6): δ (ppm) = 115.4, 116.4, 119.8, 119.9, 120.8, 123.1, 125.1, 130.7, 131.7, 140.8, 152.8, 154.1.

EI-MS (70 eV): m/z (%) = 330.6 (M+•).

3.1.2. Synthesis of sorafenib (SOR)

The characterization of SOR is described as below.

White solid, Mp: 218°C, IR (KBr): υ (cm-1) = 3300-3100 (3NH), 1707 (C=O), 1615 (C=O)

1H NMR (DMSO-d6): δ (ppm) = 2.84 (d, 3J=4.5Hz, 3H, NHCH3), 7.17 (d, 3J= 8Hz, 2H-Ar), 7.33 (dd, 3J=6.5Hz, 4J=2.5Hz, 1H-Ar), 7.59 (d, 3J=8Hz, 2H-Ar), 7.60 (d, 3J=8Hz, 1H-Ar), 7.70 (dd, 3J=8Hz, 4J=2.5Hz, 1H-Ar), 7.77 (d, 4J=2.5Hz, 1H-Ar), 8.1 (d, 4J=2.5Hz, 1H-Ar), 8.61 (d, 3J=6.5Hz, 1H-Ar), 9.17 (brd, 3J=4.5Hz, NHCH3), 9.39 (s, 1H, NH), 9.56 (s, 1H, NH).

13C NMR (DMSO-d6): δ (ppm) = 25.7, 109.9, 114.05, 116.08, 119.7, 120.7, 121.1, 121.7, 122.3, 123.3, 131.4, 137.3, 138.07, 138.9, 146.5, 146.8, 151.8, 160.3, 168.3.

EI-MS (70 eV): m/z (%) = 4.64.2 (M+•).

3.1.3. Synthesis of sorafenib tosylate (SORt) as the final product

The characteristic of SORt, which is the final product, is described as below **(Figures 1 and 2).**

White solid, Mp: 223 °C, IR (KBr): υ (cm-1) = 3500-2500 (NH and OH), 1723 (C=O), 1689 (C=O), 1598 (S=O), 1556 (S=O).

1H NMR (DMSO-d6): δ (ppm) = 2.29 (s, 3H, CH3), 2.84 (d, 3J=4.5Hz, 3H, NHCH3), 7.17 (d, 3J= 8Hz, 2H-Ar), 7.22 (d, 3J=9Hz, 2H-Ar), 7.33 (dd, 3J=6.5Hz, 4J=2.5Hz, 1H-Ar), 7.59 (d, 3J=8Hz, 2H-Ar), 7.60 (d, 3J=8Hz, 1H-Ar), 7.67 (d, 3J=9Hz, 2H-Ar), 7.70 (dd, 3J=8Hz, 4J=2.5Hz, 1H-Ar), 7.77 (d, 4J=2.5Hz, 1H-Ar), 8.1 (d, 4J=2.5Hz, 1H-Ar), 8.61 (d, 3J=6.5Hz, 1H-Ar), 9.17 (brd, 3J=4.5Hz, NHCH3), 9.39 (s, 1H, NH), 9.56 (s, 1H, NH), 13.13 (brs, 1H, OH).

13C NMR (DMSO-d6): δ (ppm) = 20.2, 25.7, 109.9, 114.05, 116.08, 119.7, 120.7, 121.1, 121.7, 122.3, 123.3, 124.9, 127.8, 131.4, 137.3, 138.07, 138.9, 143.7, 146.5, 146.8, 147.7, 151.8, 160.3, 168.3.

EI-MS (70 eV): m/z (%) = 4.64.2 (M+•).

3.2. Bioassays for anticancer activity of SORt

After the synthesis and characterization of SORt, its anticancer activity was investigated. For this subject, two cell lines of HCT116 and CT26 were selected. These cell lines have epithelial cell morphology and are rapid-growing [22, 23]. The results of the cytotoxicity assay show that CT26 cells are more sensitive to SORt than HCT116 cells, the IC50 values were also 5.42 and 8.12 μM, respectively. The results of IC50 calculation for anticancer the drug of regorafenib as positive control exhibited 17.40 and 28.62 μM for CT26 and HCT116 cells, respectively **(Fig. 3).** Considering the anticancer effects of SORt, a summarization of another study has been represented; Yao, et al. after design, synthesis and antiproliferative activity of a collection of SOR derivatives, demonstrated that one of the derivatives shown

more potent effect than that of SOR. Furthermore, two compounds have almost the same impact as SOR and the rest have less effect than SOR. In their study, the IC50 value for SORt for the HCT116 cell line was 7.8 ± 1.1, which is closer to our results [2].

3.3. Study of the interaction between SORt and BLG

3.3.1. Fluorescence measurement study

The interaction of SORt with BLG was investigated using fluorescence spectroscopy. This technique can provide information on the binding of a small molecule to the protein, such as intermolecular distances, binding sites, binding modes, binding constants, and binding mechanisms [24]. BLG has two tryptophan residues (Trp) and four tyrosine (Tyr) residues per monomer [25]. They are as aromatic amino acids and contribute to the fluorescence emission of BLG. **Fig. 4A** depicts the variation of the emission intensity of BLG solution with addition to different concentrations of SORt. The emission spectra of BLG displayed a peak at 317 nm. The addition of different concentrations of SORt to the fixed concentration of BLG resulted in a significant quenching in the fluorescence intensity. The quenching takes place when the SORt is sufficiently close to the fluorescence residues of the BLG. So, it can be concluded that several parameters such as ground state complex formation, collisional quenching, reactions in the excited-state, rearrangement of molecules and energy transfer between the ligand and the macromolecule have been occurred in the system.

3.3.2. Calculation of the binding constants between BLG and SORt

Generally, fluorescence quenching is not out of two states; they are static or dynamic. Dynamic quenching relies on intermolecular collision in a fluid environment, while static quenching depends on forming a stable ground state complex [26]. The type of quenching caused by SORt on BLG can be estimated from the variation of the quenching signal with

temperature. For this reason, the fluorescence quenching data were analyzed by the well-known Stern–Volmer equation:

$$\frac{F_0}{F} = 1 + K_q\tau_0[Q] = 1 + K_{SV}[Q]$$

The fluorescence intensities before and after the addition of SORt, are F_0 and F ,respectively. kq, τ_0, [Q] and Ksv respectively are the Stern–Volmer dynamic quenching constant, the average life-time of the biomolecule without quencher ($\tau_0=10^{-8}$ s), the concentration of the SOR, and the quenching rate constant of the biomolecule. To study the fluorescence quenching mechanism, we investigated the fluorescence quenching effect of The Stern–Volmer curves of F_0/F versus [Q] at temperatures of 298, 305 and 310 **(Fig. 4B)** [27]. The calculated of the Ksv and kq are summarized in table 1. The results represented at table 1 indicate that the quenching procedure is initiated by astatic quenching because rate constants decrease with increasing temperature. In addition, the quenching constant for BLG-SORt complex is greater than 2.0×10^{10} M s^{-1} (24.45×10^{12} M s^{-1}). This shown that fluorescence quenching does not follow the dynamic collision quenching, and most probably, a static mechanism is responsible for the formation of the complex [28, 29]. Furthermore, the Ksv values for the interactions of the SORt with BLG at different temperatures decreased with increasing temperature; confirming the static interaction between the drug and the protein.

The binding constant and the number of binding sites of SORt on BLG were calculated by the Hill equation [30]:

$$\frac{Log(F - F_0)}{F} = LogK_b + nLog[Q]$$

where F_0, F, K_b and n respectively are the fluorescence intensities without and with enhancer, the binding constant and the number of binding sites. The binding constant K_b and n at three different temperatures (298, 305 and 310) were calculated from the intercept and slope of the plot of log ($F-F_0/F$) versus log [Q], respectively [31] **(Fig. 4C)** (Table 1).

3.3.3. Determination of the thermodynamic parameters

To further characterization of the interaction forces between SOR and BLG, the thermodynamic parameters were analyzed. The thermodynamic parameters of standard Gibbs free energy change (ΔG), standard enthalpy change (ΔH) and standard entropy change (ΔS) can donate valuable information including hydrogen bonds, van der Waals force, electrostatic force, hydrophobic interaction force, which are mainly interaction forces between a drug molecule and bio-macromolecule. The binding of proteins with drug molecules can be concluded from the thermodynamic parameters: if ΔH > 0 and ΔS > 0 the main binding forces are hydrophobic interaction, ΔH < 0 and ΔS < 0 the main binding forces are van der Waals or hydrogen bond interactions and ΔH < 0 and ΔS > 0 hydrogen bonds and hydrophobic interactions are important forces for the formation of the complex. Moreover, the negative symbol in ΔG values reveals the spontaneous nature of the reaction process [32]. In this study, the thermodynamic parameters were calculated via the van't Hoff equation:

$$Ln\,K = -\frac{\Delta H}{RT} + \frac{\Delta S}{R}$$

where K is the binding constant, T is the absolute temperature, and R is the universal gas constant (8.314 J mol^{-1} K^{-1}). ΔH and ΔS were obtained from the slope and intercept of the linear plot based on lnK versus 1/T **(Fig 4D).** The free energy change (ΔG) is estimated from the following equation [33, 34]:

$$\Delta G = \Delta H - T\Delta S$$

The values of ΔH, ΔS, and ΔG for SORt binding to BLG are listed in Table 1. The negative values of ΔH, ΔS and ΔG suggested that van der Waals and hydrogen bond interactions were

the main binding forces in the interaction process between SORt and BLG, and has been occurred a spontaneous nature of the reaction process.

3.3.4. Synchronous fluorescence spectroscopy

Synchronous fluorescence spectroscopy is a useful technique to consider the microenvironment of amino acid residues through observing the maximum fluorescence wavelength shift corresponding to the polarity variation nearby the fluorophore (Tyr and Trp) molecules [35]. Therefore, the conformation changes in protein structure are determined by this method [36]. When difference values ($\Delta\lambda$) between the excitation and emission wavelengths are 15 and 60 nm, the synchronous fluorescence spectra display characteristics of the Tyr and Trp residues of the protein, respectively [37]. The results showed that, when the concentrations of SORt increase, the maximum emission wavelength in $\Delta\lambda = 60$ becomes slightly red-shifted (from 338 to 341 nm), while in $\Delta\lambda = 15$ do not appear any significant shift in that **(Figures 5A and 5B)**. This indicates that the conformation of the Trp micro-environment is changed, while for Tyr the microenvironment remained unaffected. This protein contains two residues of tryptophan (Trp-19 and Trp-61), which Trp-19 is placed on the beta-strand A and inside the beta-barrel; Trp-61 is located on the beta-strand C on the outer surface of the CD loop and is exposed to solvent [38]. The red-shift implies that the microenvironment of the Trp residues of the protein in the near the interaction site of the drug is perturbed, leading to a higher degree of exposure to the more polar aqueous environs [39].

3.3.5. Three-dimensional (3D) fluorescence spectra

When the excitation wavelength, emission wavelength and fluorescence intensity as three critical parameters in fluorescence spectroscopy be used in one axes, a new spectrum is being created, which known as 3D fluorescence spectra [40]. Because the contour map gives us valuable information such as shift at the excitation or emission wavelength around the fluorescent peak; the advent of a new peak; vanishing of the existing peak, this spectrum was

chosen to monitor the conformational changes in the BLG under interaction with SORt [41]. There are two peaks in the 3D fluorescence spectra (peaks 1 and 2). Peak 1, which is seen in the λex = 280 nm and λem = 340 nm and mostly shows the spectra behavior of the Trp and Tyr residues. Peak 2, that appeared during λex = 235 nm and λem = 337 are related to the fluorescence spectra behavior of the polypeptide backbone structure of BLG **(Figures 5C and 5D).** From the data obtained from 3D fluorescence, it can be said that the interaction between BLG and SORt is formed, and this interaction has altered the 3D structure of the BLG. Although 3D fluorescence data cannot quantify the content of α-helix, β-sheet and random coil, it can qualitatively confirm the conformational change in the protein structure.

3.3.6. Circular dichroism (CD) analysis

Generally, the interaction of the small molecules with protein cause changes in the protein polypeptide backbone conformation (secondary structure). One way to observe these changes is to use CD spectroscopy techniques. **Fig. 6A** shows the CD spectra of the BLG free and BLG-SORt system. After analyzing the data using CD analysis using Neural (CDNN) Networks, the fractions of α-helix, β-sheet and the random coil of BLG without and with SORt are listed in Table 2. As can be seen from the data in Table 2, the free BLG comprised 20.34% α-helix, 43.85% β-sheet, 35.80% random coil. Our results showed the amount of α-helix remains almost constant in the BLG–SOR system, whereas those of random coil decreased. Additionally, the content of the β-sheet was slightly increased by the addition of two amounts (5 and 10 μM) of SORt. Changes in the percentage of β-sheet and random coil structures in BLG showed that SOR bind to the amino acid residues of the main polypeptide chain of BLG.

3.3.7. Zeta-Potential Measurements

The surface properties of proteins have essential factors in their ionic interactions with other molecules. The ionization of surface groups of the proteins mainly causes the surface charge on the proteins. The surface charge of proteins can be measured using a zeta-potential technique [43]. A result of the zeta potential, which shows the effect of the addition of SORt on the BLG, is illustrated in **Fig. 6B**. As the SORt concentration increases, the zeta-potential values are also increased, which suggests the formation of BLG–SORt complex. This tendency is indicative of the existence of electrostatic interactions between BLG and SORt [44].

3.3.8. Molecular Docking

Molecular simulation is a useful technique to identify the binding site, understand and interpret the mechanism of interaction between the BLG is sorafenib. It is also used as an in silico tool to validate experimental interpretations [45]. In general, there are three major binding sites in the BLG structure, an internal cavity of the β-barrel (central calyx domain), a groove between the α-helix and the β-barrel that forms the hydrophobic surface pocket and the outer surface near Trp19-Arg124 [39]. The docking result showed that, sorafenib is unable to enter the cavity of β-barrel, and its interaction is close to the β-sheet and α-helix **(Fig 7A).** The binding of SORt to the protein is via hydrogen bonds and electrostatic forces. Hence, there is hydrogen bonding interaction between SORt and BLG through the residue Asp53, which is consistent with the results of thermodynamics parameters. Furthermore, the charged amino acids of Asp53, Glu74, Lys75, Lys83 and Asp85 participate in the formation of electrostatic interactions **(Fig 7B),** which confirms the results obtained from zeta potential measurements.

4. Conclusion

Since the SORt is one of the most widely used drugs among cancer patients, it was successfully synthesized in this project, and its anticancer properties was confirmed against

two colon cancer cell lines of HCT116 and CT26. In general, SORt is a small molecule with the hydrophobic nature; hence it is a limiting factor for its oral administration. One way to overcome this limitation is to use a carrier that can form a complex with the drug. So, in this study dietary protein of β-lactoglobulin (BLG) was used for this purpose, and its interaction with the drug was investigated. Stern–Volmer dynamic quenching constant (kq), steady-state and fluorescence resonance energy transfer (FRET) results showed that static quenching is the primary reason for fluorescence quenching of BLG in complex with SORt. The negative values of thermodynamic parameters, including ΔH and ΔS suggested that van der Waals and hydrogen bond interactions were the main binding forces in the system of BLG-SORt. Circular dichroism exhibited that the amount of α-helix remains almost constant in the BLG–SORt complex. Thus, it became apparent that SORt high affinity can bind to a suitable site at the BLG protein surface. Therefore, based on the insights into drug and protein binding, in the future studies we are looking for the design of nanoparticles of SORt based on BLG protein.

Disclosure statement

No potential conflict of interest was reported by the authors.

Acknowledgement

This work is a part of a research project and was financially supported by Deputy of Research, Hamadan University of Medical Sciences [Grant number: 9704192187]. Therefore, the authors are very thankful for the support of this deputy.

References

1. Siegel, R.L., K.D. Miller, and A. Jemal, *Cancer statistics, 2019.* CA: a cancer journal for clinicians, 2019. **69**(1): p. 7-34.

2. Yao, J., et al., *Design, synthesis and biological activities of sorafenib derivatives as antitumor agents.* Bioorganic & medicinal chemistry letters, 2012. **22**(21): p. 6549-6553.

3. Morgillo, F., et al., *Antitumor activity of sorafenib in human cancer cell lines with acquired resistance to EGFR and VEGFR tyrosine kinase inhibitors.* PLoS One, 2011. **6**(12).

4. Agarwal, S., et al., *The role of the breast cancer resistance protein (ABCG2) in the distribution of sorafenib to the brain.* Journal of Pharmacology and Experimental Therapeutics, 2011. **336**(1): p. 223-233.

5. Swain, B.C., et al., *Biophysical study on complex formation between β-Lactoglobulin and vitamin B12.* Food Chemistry, 2020. **312**: p. 126064.

6. Albani, J.R., et al., *Tryptophan 19 residue is the origin of bovine β-lactoglobulin fluorescence.* Journal of pharmaceutical and biomedical analysis, 2014. **91**: p. 144-150.

7. Maity, S., et al., *Multispectroscopic analysis and molecular modeling to investigate the binding of beta lactoglobulin with curcumin derivatives.* RSC Advances, 2016. **6**(113): p. 112175-112183.

8. Shafaei, Z., et al., *β-Lactoglobulin: An efficient nanocarrier for advanced delivery systems.* Nanomedicine: Nanotechnology, Biology and Medicine, 2017. **13**(5): p. 1685-1692.

9. Izadi, Z., et al., *β-lactoglobulin–pectin Nanoparticle-based Oral Drug Delivery System for Potential Treatment of Colon Cancer.* Chemical biology & drug design, 2016. **88**(2): p. 209-216.

10. Liang, L. and M. Subirade, *β-Lactoglobulin/folic acid complexes: formation, characterization, and biological implication.* The Journal of Physical Chemistry B, 2010. **114**(19): p. 6707-6712.

11. Gholami, H., et al., *The simultaneous carrier ability of natural antioxidant of astaxanthin and chemotherapeutic drug of 5-fluorouracil by whey protein of β-*

lactoglobulin: spectroscopic and molecular docking study. Journal of Biomolecular Structure and Dynamics, 2020: p. 1-13.

12. Bijari, N., S. Ghobadi, and K. Derakhshandeh, *Irinotecan binds to the internal cavity of beta-lactoglobulin: A multi-spectroscopic and computational investigation.* Journal of pharmaceutical and biomedical analysis, 2017. **139**: p. 109-115.

13. Moradi, M., et al., *Remarkable apoptotic pathway of Hemiscorpius lepturus scorpion venom on CT26 cell line.* Cell biology and toxicology, 2019: p. 1-13.

14. Moradi, M., et al., *Determining Optimal Cell Density and Culture Medium Volume simultaneously in MTT Cell Proliferation Assay for Adherent Cancer Cell Lines.* Helix, 2018. **8**(2): p. 3274-3280.

15. Mahdavinejad, L., et al., *Extremely low frequency electromagnetic fields decrease serum levels of interleukin-17, transforming growth factor-β and downregulate Foxp3 expression in the spleen.* Journal of Interferon & Cytokine Research, 2018. **38**(10): p. 457-462.

16. Tanzadehpanah, H., et al., *Human serum albumin binding and synergistic effects of gefitinib in combination with regorafenib on colorectal cancer cell lines.* Colorectal Cancer, 2018. **7**(2): p. CRC03.

17. Tanzadehpanah, H., et al., *Binding site identification of anticancer drug gefitinib to HSA and DNA in the presence of five different probes.* Journal of Biomolecular Structure and Dynamics, 2018: p. 1-14.

18. Mahaki, H., et al., *Cytotoxicity and antioxidant activity of Kamolonol acetate from Ferula pseudalliacea, and studying its interactions with calf thymus DNA (ct-DNA) and human serum albumin (HSA) by spectroscopic and molecular docking techniques.* Process Biochemistry, 2018.

19. Mahaki, H., et al., *Interaction between ropinirole hydrochloride and aspirin with human serum albumin as binary and ternary systems by multi-spectroscopic, molecular modeling and zeta potential.* Journal of Luminescence, 2013. **134**: p. 758-771.

20. Wani, T.A., et al., *Spectroscopic and molecular modeling studies of binding interaction between bovine serum albumin and roflumilast.* Drug design, development and therapy, 2018. **12**: p. 2627.

21. Kharazmi-Khorassani, J., A. Asoodeh, and H. Tanzadehpanah, *Antioxidant and angiotensin-converting enzyme (ACE) inhibitory activity of thymosin alpha-1 (Thα1) peptide.* Bioorganic chemistry, 2019. **87**: p. 743-752.

22. Samadi, P., et al., *Let-7e enhances the radiosensitivity of colorectal cancer cells by directly targeting insulin-like growth factor 1 receptor.* Journal of cellular physiology, 2019. **234**(7): p. 10718-10725.

23. Kohlan, A.K., et al., *Induction of let-7e gene expression attenuates oncogenic phenotype in HCT-116 colorectal cancer cells through targeting of DCLK1 regulation.* Life sciences, 2019. **228**: p. 221-227.

24. Millan, S., et al., *Interaction of lysozyme with rhodamine B: a combined analysis of spectroscopic & molecular docking.* Journal of Photochemistry and Photobiology B: Biology, 2016. **162**: p. 248-257.

25. Moghadam, N.H., et al., *In vitro cytotoxicity and DNA/HSA interaction study of triamterene using molecular modelling and multi-spectroscopic methods.* Journal of Biomolecular Structure and Dynamics, 2018: p. 1-12.

26. Swain, B.C., et al., *A spectroscopic and computational intervention of interaction of lysozyme with 6-mercaptopurine.* Analytical and Bioanalytical Chemistry, 2020: p. 1-13.

27. Rout, J., et al., *Spectroscopic insight into the interaction of dopamine with spherical gold nanoparticles.* Journal of Photochemistry and Photobiology B: Biology, 2020. **203**: p. 111770.

28. Wani, T.A., et al., *Study of the interactions of bovine serum albumin with the new anti-inflammatory agent 4-(1, 3-Dioxo-1, 3-dihydro-2H-isoindol-2-yl)-N'-[(4-ethoxy-phenyl) methylidene] benzohydrazide using a multi-spectroscopic approach and molecular docking.* Molecules, 2017. **22**(8): p. 1258.

29. Wani, T.A., et al., *Study of interactions of an anticancer drug neratinib with bovine serum albumin: spectroscopic and molecular docking approach.* Frontiers in chemistry, 2018. **6**: p. 47.

30. Tanzadehpanah, H., et al., *Improving efficiency of an angiotensin converting enzyme inhibitory peptide as multifunctional peptides.* Journal of Biomolecular Structure and Dynamics, 2018. **36**(14): p. 3803-3818.

31. Wani, T.A., et al., *Evaluation of competitive binding interaction of neratinib and tamoxifen to serum albumin in multidrug therapy.* Spectrochimica Acta Part A: Molecular and Biomolecular Spectroscopy, 2020. **227**: p. 117691.

32. Wani, T.A., et al., *Study of binding interaction of rivaroxaban with bovine serum albumin using multi-spectroscopic and molecular docking approach.* Chemistry Central Journal, 2017. **11**(1): p. 1-9.

33. Zhang, H.-x., H.-x. Xiong, and L.-w. Li, *Investigation on the protein-binding properties of icotinib by spectroscopic and molecular modeling method.* Spectrochimica Acta Part A: Molecular and Biomolecular Spectroscopy, 2016. **161**: p. 88-94.

34. Wani, T.A., et al., *Spectrophotometric and molecular modelling studies on in vitro interaction of tyrosine kinase inhibitor linifanib with bovine serum albumin.* PLoS One, 2017. **12**(4): p. e0176015.

35. Alanazi, M.M., et al., *Mechanistic interaction study of 5, 6-Dichloro-2-[2-(pyridin-2-yl) ethyl] isoindoline-1, 3-dione with bovine serum albumin by spectroscopic and molecular docking approaches.* Saudi Pharmaceutical Journal, 2019. **27**(3): p. 341-347.

36. Ye, Z.-w., et al., *A spectroscopic study on the interaction between the anticancer drug erlotinib and human serum albumin.* Journal of Inclusion Phenomena and Macrocyclic Chemistry, 2014. **78**(1-4): p. 405-413.

37. Chen, Y.-C., et al., *Binding between saikosaponin C and human serum albumin by fluorescence spectroscopy and molecular docking.* Molecules, 2016. **21**(2): p. 153.

38. Ghalandari, B., et al., *β-Lactoglobulin nanoparticle as a chemotherapy agent carrier for oral drug delivery system.* Journal of the Iranian Chemical Society, 2015. **12**(4): p. 613-619.

39. Sneharani, A.H., et al., *Interaction of curcumin with β-lactoglobulin stability, spectroscopic analysis, and molecular modeling of the complex.* Journal of agricultural and food chemistry, 2010. **58**(20): p. 11130-11139.

40. Al-Mehizia, A.A., et al., *Evaluation of Biophysical Interaction between Newly Synthesized Pyrazoline Pyridazine Derivative and Bovine Serum Albumin by Spectroscopic and Molecular Docking Studies.* Journal of Spectroscopy, 2019. **2019**.

41. Zhang, G., et al., *Study of the interaction between icariin and human serum albumin by fluorescence spectroscopy.* Journal of Molecular Structure, 2008. **881**(1-3): p. 132-138.

42. Swain, B.C., et al., *Monitoring the binding of serotonin to silver nanoparticles: a fluorescence spectroscopic investigation.* Journal of Photochemistry and Photobiology A: Chemistry, 2018. **367**: p. 219-225.

43. Jenkins, S.V., et al., *Understanding the interactions between porphyrin-containing photosensitizers and polymer-coated nanoparticles in model biological environments.* Journal of colloid and interface science, 2016. **461**: p. 225-231.

44. Memarpoor-Yazdi, M. and H. Mahaki, *Probing the interaction of human serum albumin with vitamin B2 (riboflavin) and L-Arginine (L-Arg) using multi-spectroscopic, molecular modeling and zeta potential techniques.* Journal of Luminescence, 2013. **136**: p. 150-159.

45. Bahmani, A., et al., *Introducing a pyrazolopyrimidine as a multi-tyrosine kinase inhibitor, using multi-QSAR and docking methods.* Molecular Diversity, 2020: p. 1-17.

Graphical Abstract

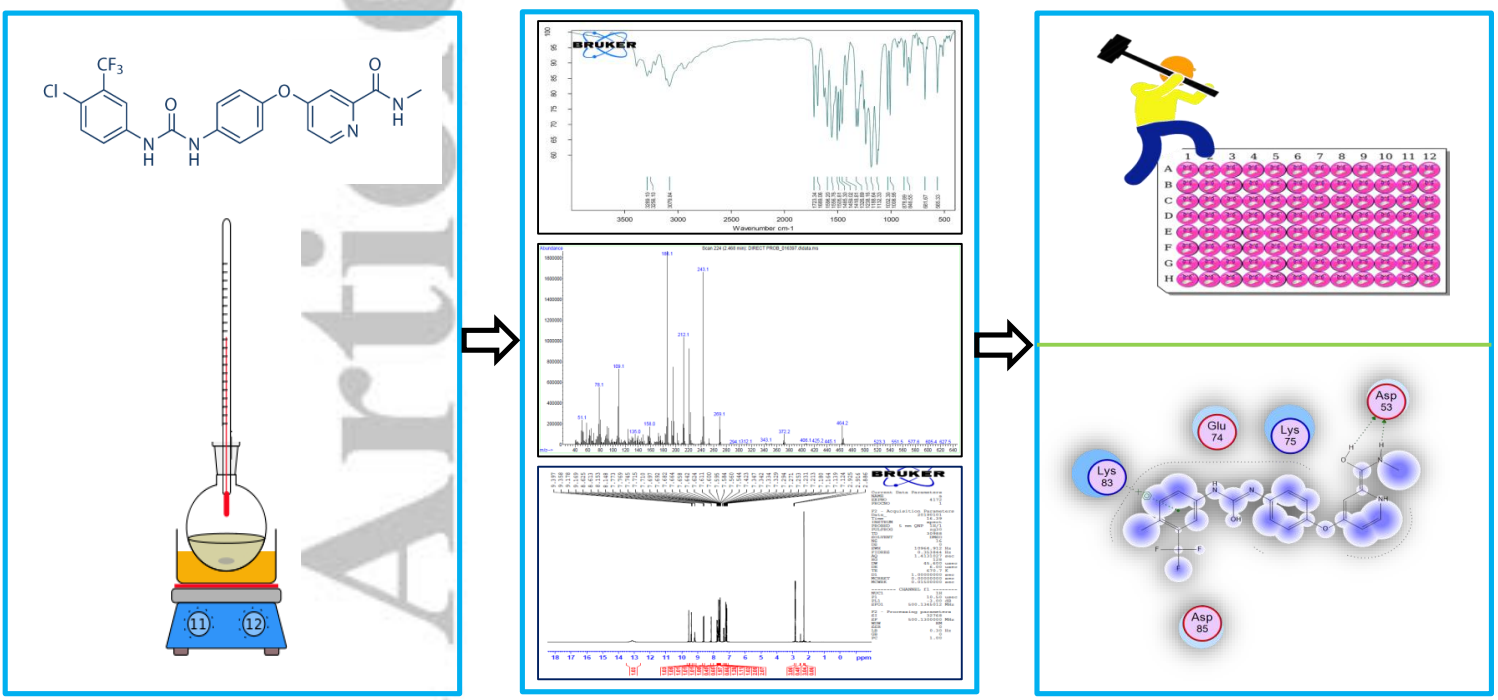

1- Synthesis of Sorafenib

2- Confirmed by FT-IR, Mass and NMR

3- Sorafenib Cytotoxicity on HCT116 & CT26 and its Binding to β-lactoglobulin

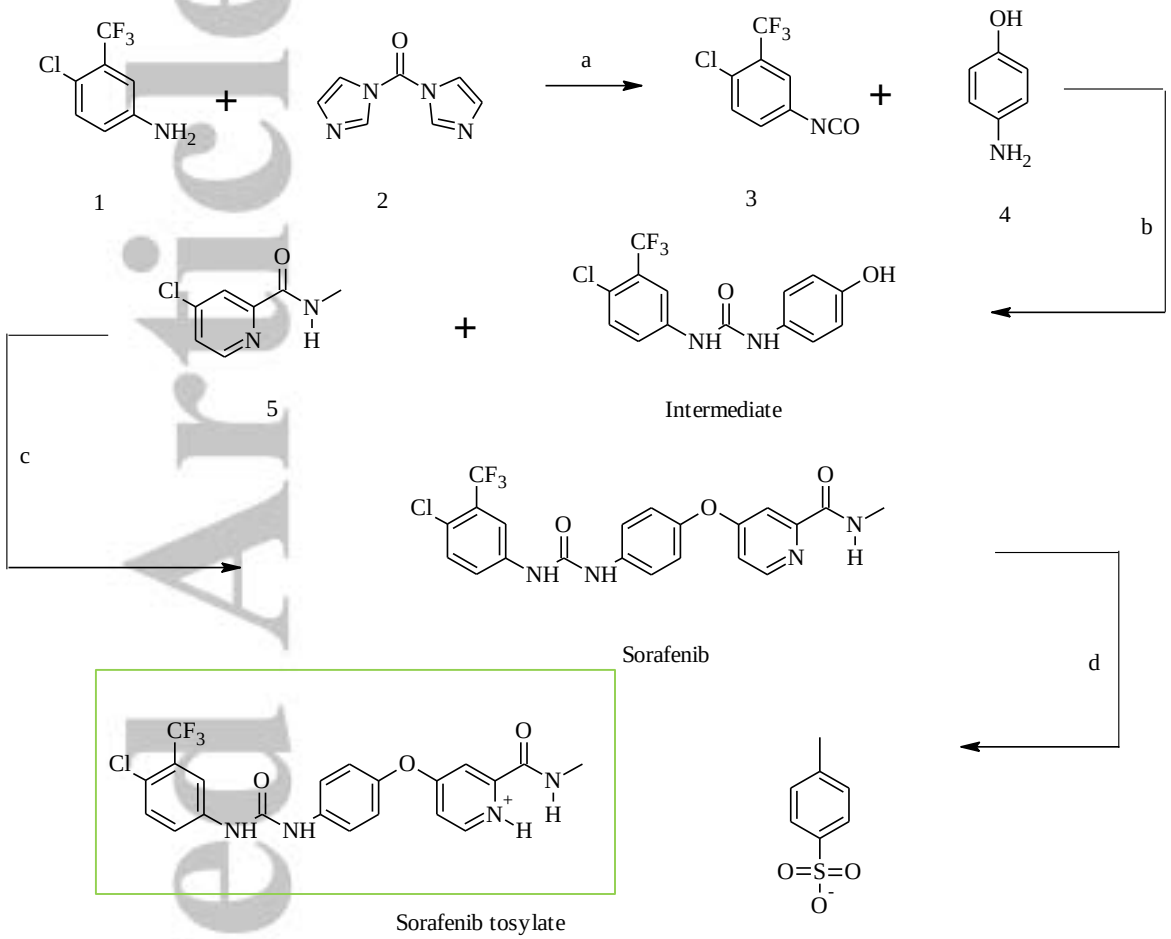

Scheme 1. Synthesis of Sorafenib tosylate, **(a)** CH_2Cl_2, reflux, 16h **(b)** CH_2Cl_2, r.t., 16h **(c)** DMF, potassium tert-butylate, K_2CO_3, 80°C, **(d)** EtOH, r.t., 15h

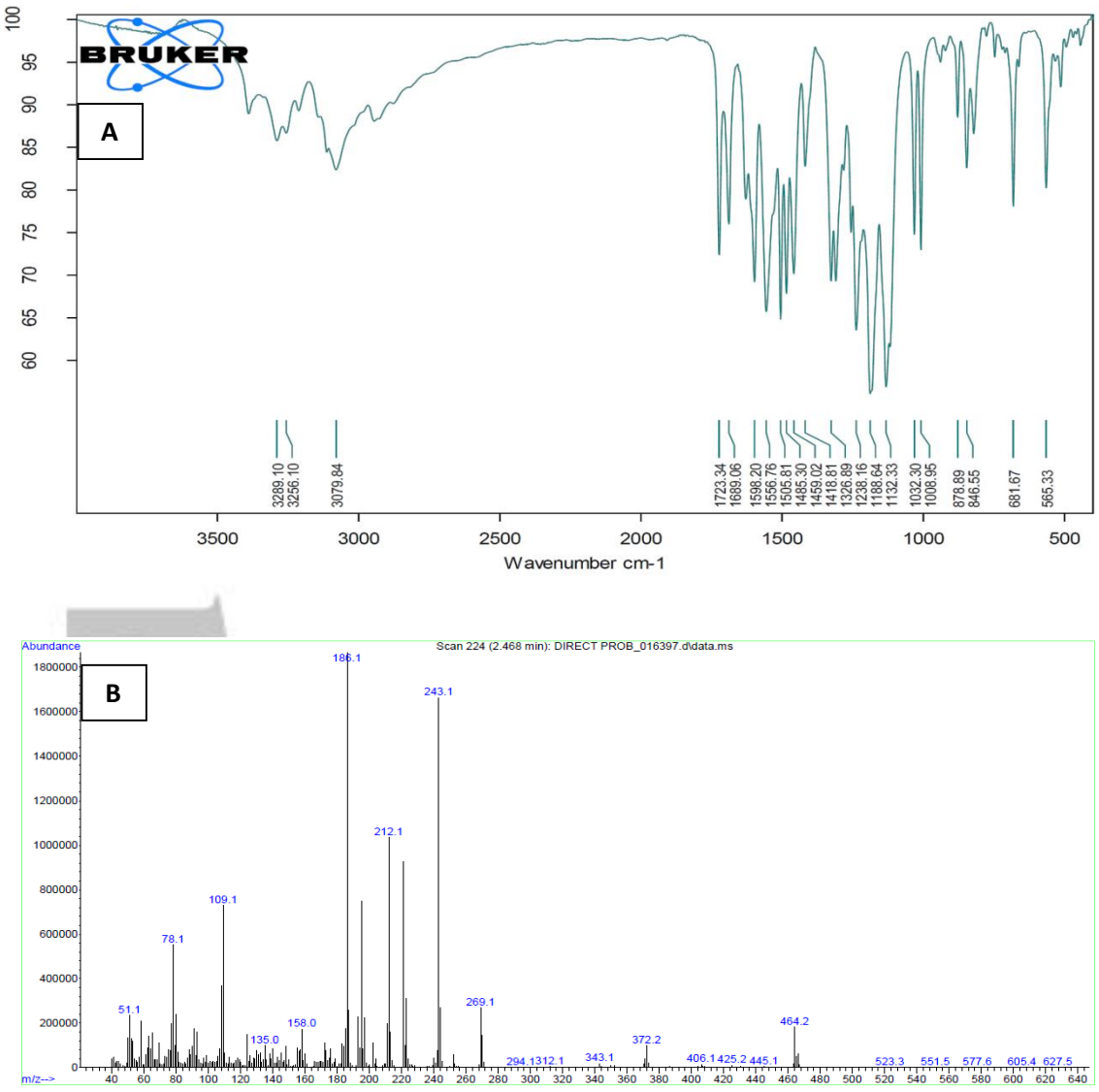

Figure 1. Sorafenib tosylate spectra IR (A) and Mass (B).

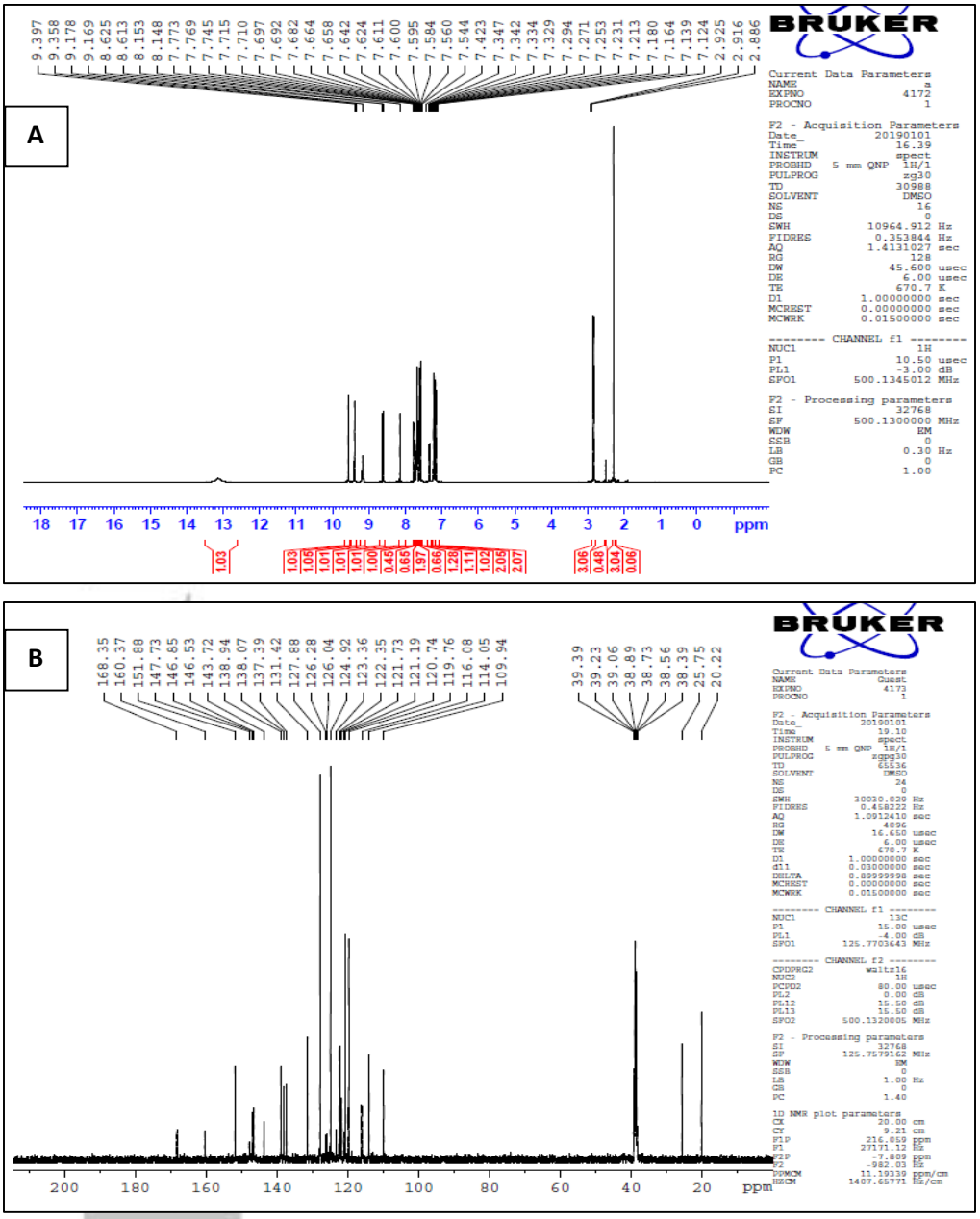

Figure 2. Sorafenib tosylate spectra ^{H}MNR (A) and ^{C}NMR (B).

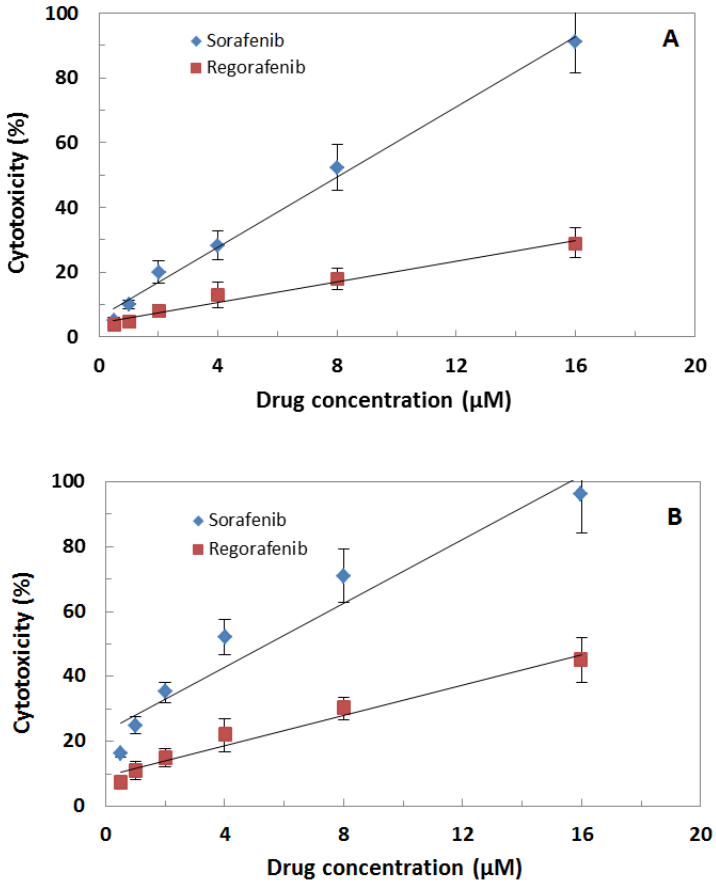

Figure 3: Cytotoxicity effects of Sorafenib tosylate and Regorafenib on two cancer cell *lines* of HCT116 **(A)** and CT26 **(B).**

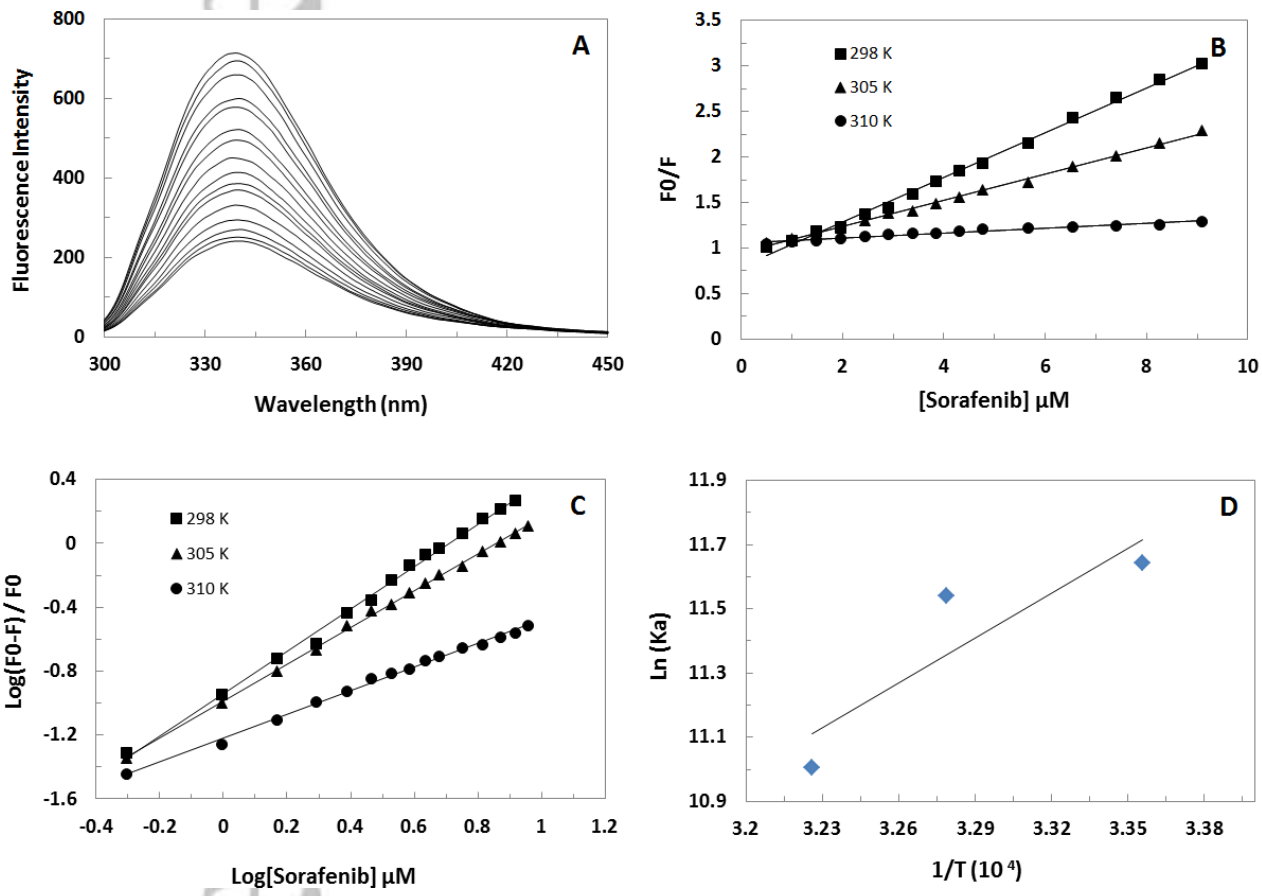

Figure 4. Fluorescence quenching, Stern–Volmer and Hill curves for the interaction between β-lactoglobulin (BLG) and Sorafenib tosylate (SORt). Fluorescence quenching of BLG (21×10^{-6} M) induced by SORt (0.0 to 10×10^{-6} M) **(A)**, Stern–Volmer curves of BLG-SORt complex at different temperatures **(B)**, Double logarithmic plots of log((F0 – F)/F) against log[SORt] derived from the fluorescence quenching at different temperatures and pH 7.4 **(C)** and van't Hoff plot for the binding of SORt with BLG (D).

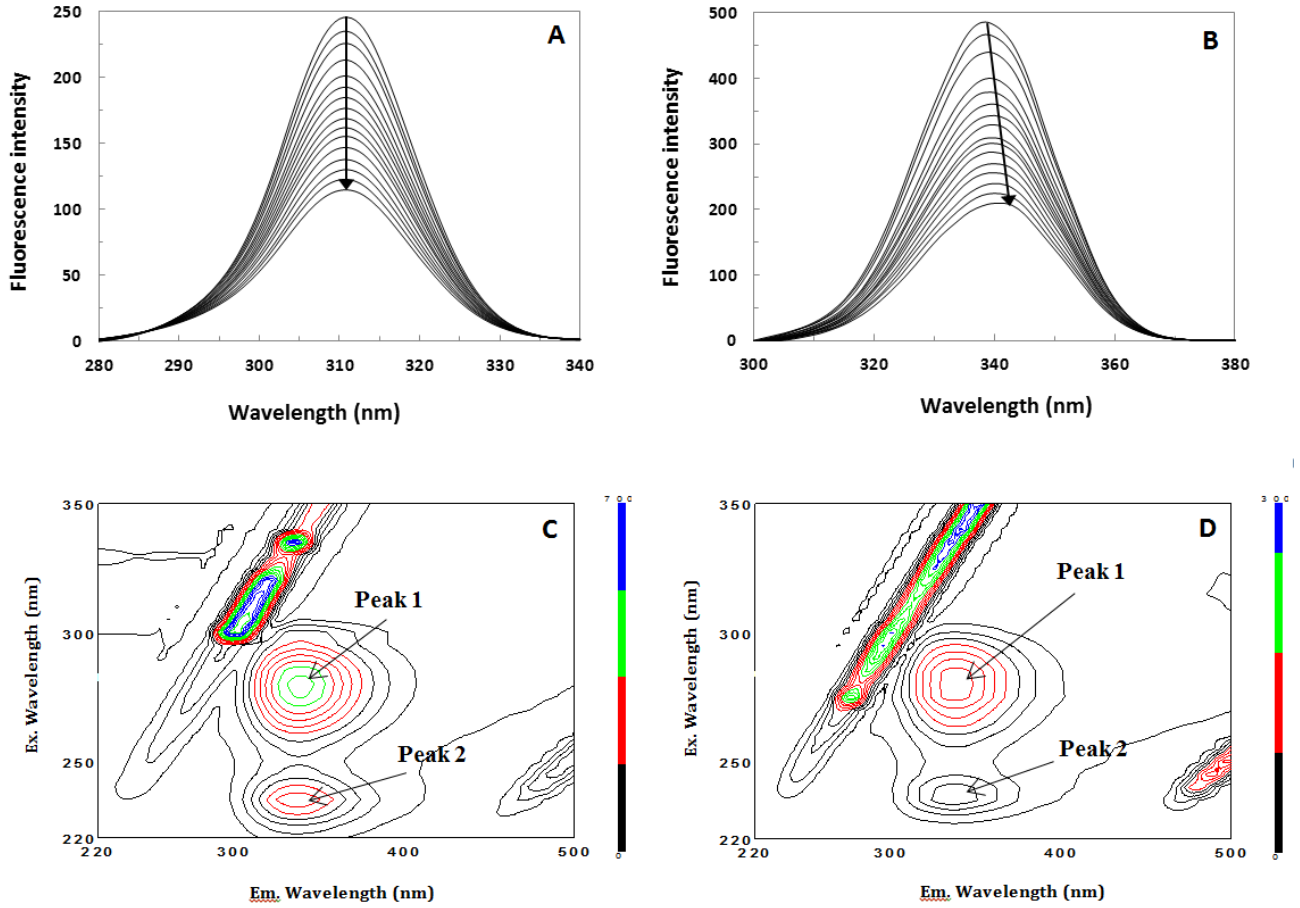

Figure 5. Synchronous and three-dimensional fluorescence spectra for the interaction between β-lactoglobulin (BLG) and Sorafenib tosylate (SORt). Synchronous fluorescence spectra of BLG (21×10^{-6} M) in the presence of increasing concentrations of SORt (0.0 to 10×10^{-6} M) at $\Delta\lambda = 15$ nm **(A)**, and $\Delta\lambda = 60$ nm **(B)**. Contour diagrams of three-dimensional fluorescence spectra of BLG free (21×10^{-6} M) **(C)**, BLG-SORt (SORt concentration 10×10^{-6} M) **(D)**. T= 298 k, pH 7.4.

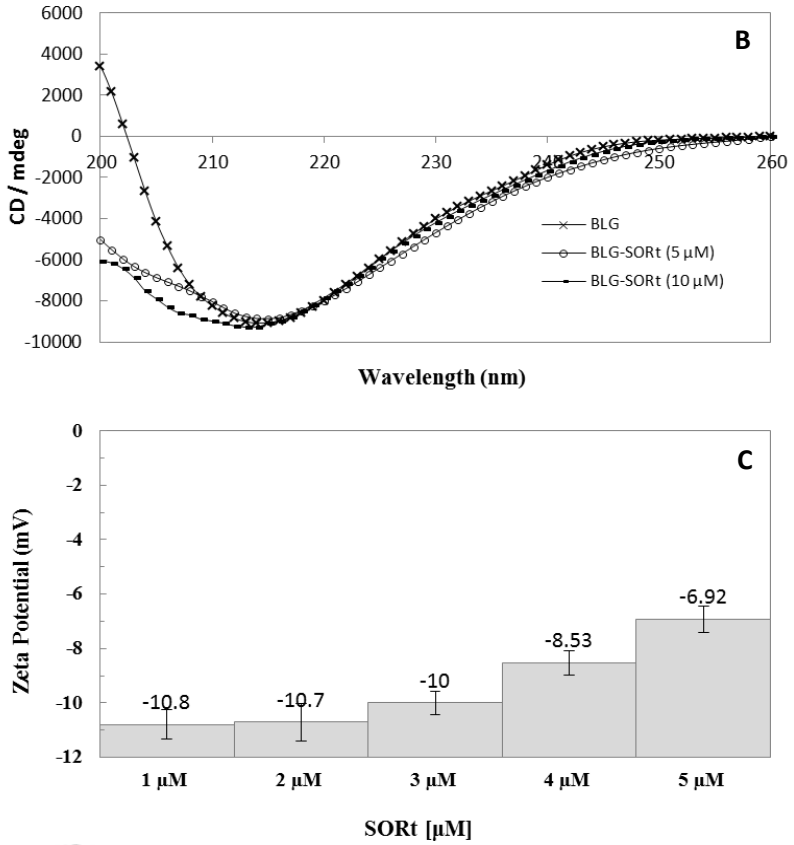

Figure 6. Circular dichroism (CD) and Zeta potential spectra for the interaction between β-lactoglobulin (BLG) and Sorafenib tosylate (SORt). CD spectra of BLG free (21×10^{-6} M) and BLG in the presence of 5 and 10×10^{-6} M of SORt **(A)**. Zeta potential spectra of BLG (21×10^{-6} M) in the absence and presence SORt, ($0.0 – 5 \times 10^{-6}$ M) **(B)**. T=298 K, pH 7.4.

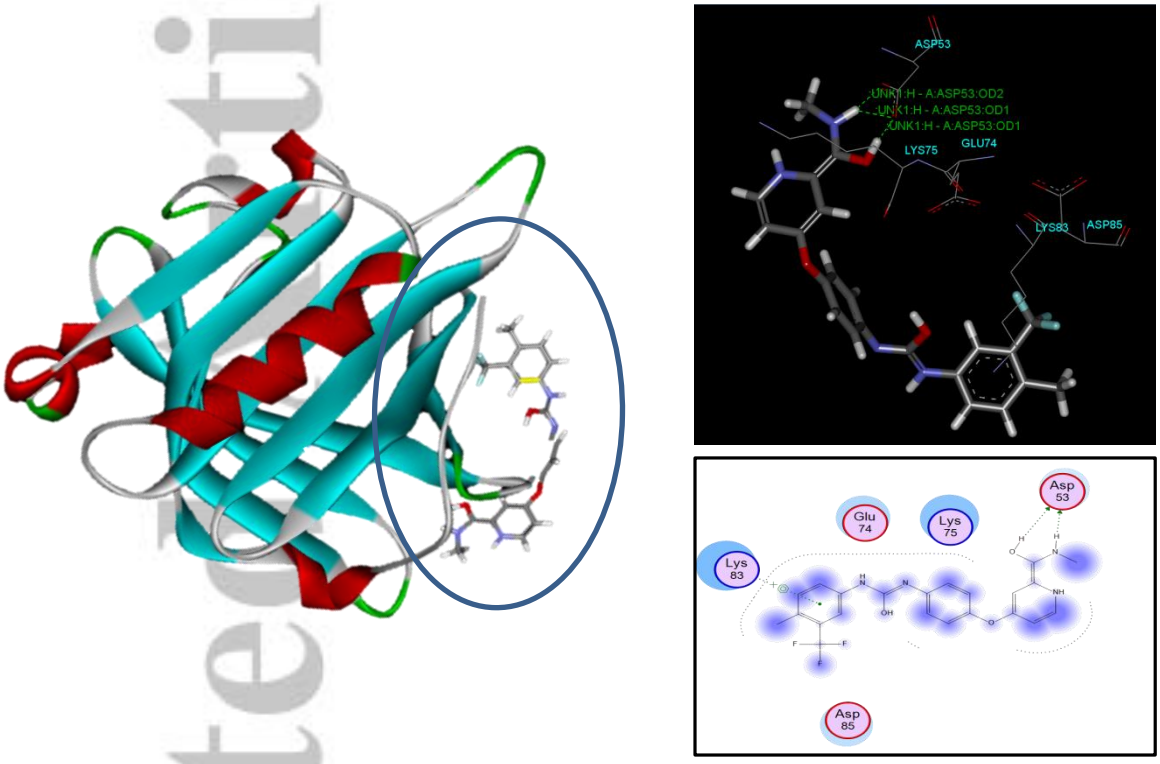

Figure 7. Molecular modeling for the interaction between β-lactoglobulin and Sorafenib tosylate. Only residues around 4 Å of drug are displayed

Table 1. The Stern–Volmer quenching constants (Ksv), quenching rate (Kq), binding constants (Kb and n) and thermodynamic parameters for the interaction between β-lactoglobulin (BLG) and Sorafenib tosylate (SORt), at different temperatures (pH 7.4).

T (K)	Ksv (M^{-1})	Kq (M^{-1})	Kb (M^{-1})	n	ΔH (kj mol-1)	ΔS (j mol-1)	ΔG (kj mol-1)
298	24.45×10^4	24.45×10^{12}	11.39×10^4	1.3			-29.025
305	14.4×10^4	14.4×10^{12}	10.27×10^4	1.15	-38.75	-32.64	-28.801
310	2.73×10^4	2.73×10^{12}	6.01×10^4	0.74			-28.638

Table 2. Secondary structure composition of the β-lactoglobulin (BLG) determined with and without Sorafenib tosylate (SORt) by CD spectroscopy.

Systems	α-helix	β-sheet	random coil
BLG free	20.34	43.85	35.80
BLG-SORt (5 μM)	20.57	46.58	32.84
BLG-SORt (10 μM)	20.44	47.73	31.82